# Numerical Investigation on Flow Control Effects of Plasma Actuators for Subsonic Aerofoils in Turbine Applications

**G. W. Bell[1], H. Ogawa[1] and S. Watkins[1]**

[1]School of Aerospace, Mechanical, and Manufacturing Engineering,
RMIT University, Melbourne, Victoria 3001, Australia

## Abstract

Plasma actuators are all electrical devices capable of altering flow paths and reattaching separated boundary layers. The application to low pressure turbine stages in axial turbine engines indicates further fuel efficiency improvements at low Reynolds numbers. Using wind tunnel experiments, a numerical plasma model through steady-state simulations with RANS turbulence modeling was developed. Reasonable agreement has been observed in the calibration of the numerical plasma model to experimental data. Further parametric studies are considered, aiming to optimize control, reduce pressure loss for turbine stages, and reduce actuator power consumption.

## Introduction

Rising markets for on-demand power generation and a larger public focus on greener air transportation are encouraging gas turbine manufacturers to develop gas turbines with greater fuel efficiencies. One possible avenue to increase the efficiency of a turbine is to minimize the pressure drop encountered over the turbine and compressor stages by maintaining coherent and attached flow around the blade cross sections. Sustaining attached flow over the blade cross sections becomes difficult when the fluid inside the turbine experiences particularly low Reynolds numbers. This can occur in cases such as (1) low density atmospheric conditions for aircraft turbines (2) high inlet temperature conditions for industrial power turbines (3) miniaturization of the compressor and turbine cascades in small scale turbines [4].

Passive flow control technologies such as fixed tabulators, vortex generators, and dimples are currently employed to trigger transition and reattach a turbulent boundary layer at low Reynolds numbers. These devices also produce undesirable drag and hence pressure and efficiency losses at higher Reynolds numbers [5]. Recent research into other active flow control methods indicate that plasma actuators may be particularly well suited to control the boundary layer on the turbine and compressor stages when desired [2].

Two separated electrodes are excited with an AC voltage and induce plasma creation during the peak voltages of the AC wave [1]. The resulting ions from the plasma collide with ambient air molecules, transferring momentum by inducing a flow away from the exposed electrode, thereby generating a net body force [2].

Plasma actuators contain no moving parts, are lightweight, thin, and fast reacting. Proof of concept experiments [6, 3] have demonstrated that for compressor and turbine applications the power requirement is on the order of 100 mW to reduce the pressure drop coefficient by 55% [5].

In 2012 Matsunuma and Segawa from AIST Japan investigated wind tunnel experiments on a pressure matched 2D turbine blade section at low Reynolds numbers [5]. A plasma actuator was placed on the suction side of a turbine pressure matched airfoil section. They observed the actuator effect in a series of experiments by varying the voltage potential with a constant AC frequency. The streamwise velocity was adjusted to produce a Reynolds number of $1.7 \times 10^4$ and the 2D flowfield was recorded using Particle Image Velocimetry (PIV). Their experimental results indicate that plasma actuators are effective methods for reattaching flow and reducing the total pressure drop experienced by turbine stages.

This investigation aims to expand on the developments of Rizzetta and Visbal in 2010 [6] using the experimental data developed by Matsunuma and Segawa in 2012 [5]. The dataset produced by Matsunuma and Segawa [5] has been selected to be used as the foundation for the validation of a 2D computational fluid dynamics (CFD) model.

## Approach

Calibration of the plasma actuator model in comparison with experiments conducted by Matsunuma and Segawa [5] is performed first. Due to limited computational power and time restraints, Reynolds Averaged Navier-Stokes (RANS) turbulence modeling is employed in steady-state simulations.

### 2-D Wall Contour

Turbomachinery in CFD is typically simulated through periodic boundary conditions between blades and vanes. Matsunuma and Segawa developed their experimental results on the suction surface of a pressure matched turbine blade using a quasi-2D pressure matched surface [5]. They state that the curved surface of the test section was designed using a one-dimensional continuity argument to match the surface velocity and pressure distribution of a corresponding turbine blade. These results are used as the validation for the initial CFD models.

### Plasma Actuator Model

The most common plasma actuator used in current literature for separation control is the asymmetric single dielectric barrier discharge (DBD) plasma actuator. The configuration of this actuator consists of two electrodes with one exposed to the air and the other completely encapsulated under an insulating dielectric material. To sustain plasma production, and hence a body force, the electrodes are typically excited with an AC frequency of around 3 - 15 kHz and voltage of typically greater than 1 kV for the electric field strength to begin ionization [2]. The relatively high kinetic energy of the newly separated positive ions and electrons then transfer kinetic energy to non-ionized air molecules, thus injecting the boundary layer with momentum [2]. The plasma model developed by Shyy, Jayaraman, and Andersson [1] is implemented first as a starting point and to validate the plasma forcing cases described by Matsunuma and Segawa in 2012 [5].

The plasma actuator forcing is applied by adding source terms to the momentum equations in each dimension. Equation (1) describes approximated electric field lines in the plasma region

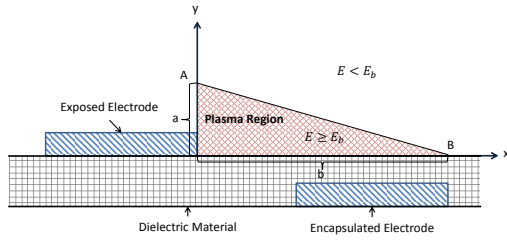$$|E| = E_0 - k_1 x - k_2 y \tag{1}$$

Figure 1. Schematic of simplified plasma modeling [1]

where $k_1$ and $k_2$ are geometric constants and can be evaluated by two simultaneous equations from the conditions that $E$ at $(0,a)$ is equal to $E_0$ and $E$ at $(b,0)$ is equal to $E_b$ (break down electric field strength). Where $E_0$ is the electric field in the region between electrodes and can be approximated as

$$E_0 = \frac{V}{d} \qquad (2)$$

where $d$ is the horizontal distance between electrodes. The plasma force per unit density at each cell is approximated by

$$F_{AVG_x} = \vartheta\alpha\rho_c e_c \Delta t E_x \qquad (3)$$

$$F_{AVG_y} = \vartheta\alpha\rho_c e_c \Delta t E_y \qquad (4)$$

where $F_{AVG_{x/y}}$ is the plasma force density experienced by the fluid at that cell location, $\vartheta$ the AC electrode frequency, $\alpha$ the ion to neutral particle collision efficiency factor, $\rho_c$ the electron charge density, $e_c$ the fluid permittivity of the electric field. $\Delta t$ is the time interval during the AC cycle where the positive voltage causes the electric field strength to cause ionization of air molecules, and $E_x$ the electric field strength at that cell in the $x$-direction.

The values selected for use in the calibration of the numerical actuator model are included in table 1.

## Computational Fluid Dynamics

The flowfields are computed utilizing the commercial code AN-SYS FLUENT[1]. No wall function is used and a small first layer height is used to maintain the $y^+$ of approximately 1, appropriate for the two-equation Shear Stress Transport (SST) $k-\omega$ RANS model. The freestream inflow is calibrated to approximately 1.1 m/s and incompressible flow is assumed utilizing a density of 1.225 kg/m$^3$ to match experimental flowfields. Energy equations are not used for incompressible flowfields. Second-order spatial accuracy was used followed by mesh adaption to reduce truncation errors to approximately $1\times10^{-4}$. A mesh sensitivity study has been performed for meshes containing 96 k, 177 k, 255 k and 315 k cells and 177 k cells has been selected for the balance between the computational expense and simulation fidelity, particularly for the boundary layer. Steady flowfields are obtained by ensuring the massflow deficit between the inlet and outlet converged to an order of $1\times10^{-8}$ and the velocity field near the trailing edge. Non-slip walls are assumed for the ceiling and floor. Conformal meshing is used for the region to apply plasma source terms.

## Results

### Physical Observations

Figure 4 displays the flowfield for the baseline plasma-on conditions. Flowfields for no and low plasma forcing conditions is dominated by massively separated flow and large recirculation

---

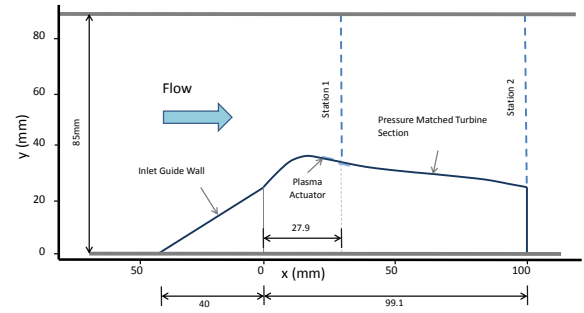[1]Developed by ANSYS inc. PA, USA.



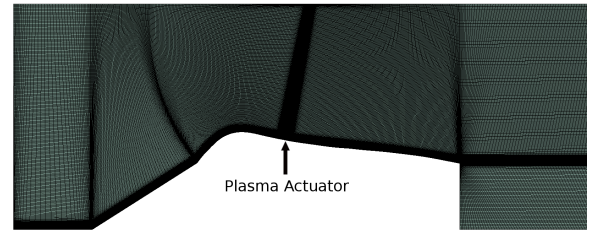Figure 2. Schematic of computational domain



Figure 3. Computational mesh

regions. The experimental case depicts large clockwise vorticies forming in the transient region between the freestream and recirculating flow. Plasma-on cases 2000 V to 2400 V show a decrease in recirculation region height. For plasma-on cases 2600 V to 2800 V the flow become reattached on the suction side and reduces separation length as voltage increases, also observed in the experimental cases [5].

### Turbulence Model Selection

Different turbulence models are applied to determine the closest qualitative response to the experimental results performed by Matsunuma and Segawa [5]. Figure 5 shows the streamwise velocity ($U_x$) m/s against the vertical position rake for the experimental results as well as the recorded flowfields of the Spalart-Allmaras, $k-\omega$ SST, and TransSST turbulence models. Other models such as the Reynolds stress five-equation model were applied but produced unrealistic separation and recirculation characteristics. The $k-\omega$ SST model is seen to provide the closest approximation to the experimental results considering the velocity gradient in the recirculation region as well as the shear layer height and freestream velocity behavior. The $k-\omega$ SST model also provides the most realistic response with regard to input turbulence properties. The TransSST model requires extremely low inflow turbulence intensity values to produce a similar separation response to the experimental velocity profile. For these reasons the $k-\omega$ SST model has been selected for the plasma-on calibration cases.

### Calibration Against Experiment

The hydraulic diameter of the duct is set to 0.04 m. The inflow velocity (1.1 m/s) and turbulence intensity (15 %) are calibrated so that the velocity measurements in the streamwise direction $U_x$ at the Stations 1, 0.0297 m, and Station 2, 0.0991 m, matched the experimental results for the baseline (plasma-off case) qualitatively well with respect to freestream velocity, shear layer height, and recirculation velocity.

The streamwise component of velocity $U_x$ in the recirculation zone (Station 2) is deemed to be the most important feature to model correctly for a qualitatively similar flowfield. The velocity profile in Figure 5 shows that the experimental data [5] is modeled qualitatively well by $k-\omega$ providing the most robust

| | | |
|---|---|---|
| AC Frequency ($\vartheta$) | 8100 | Hz |
| Collision Efficiency Coefficient ($\alpha$) | 0.4 | dimensionless |
| Electron Charge Density ($\rho_c$) | $1\times10^8$ | electrons/mm$^3$ |
| Fluid Permittivity ($e_c$) | $8.854\times10^{-9}$ | F/mm |
| Plasma Creation Time Interval ($\Delta t$) | $51.2\times10^{-6} \leq \Delta t \leq 54.6\times10^{-6}$ | seconds |
| Input Voltage ($V_{RMS}$) | $2000 \leq V_{RMS} \leq 2800$ | V |
| Break Down Electric Field Strength ($E_b$) | 3000 | V/mm |
| Distance Between Electrodes ($d$) | 0.25 | mm |
| Approximated Plasma Height ($a$), Width ($b$) | 1.5, 3.0 | mm |

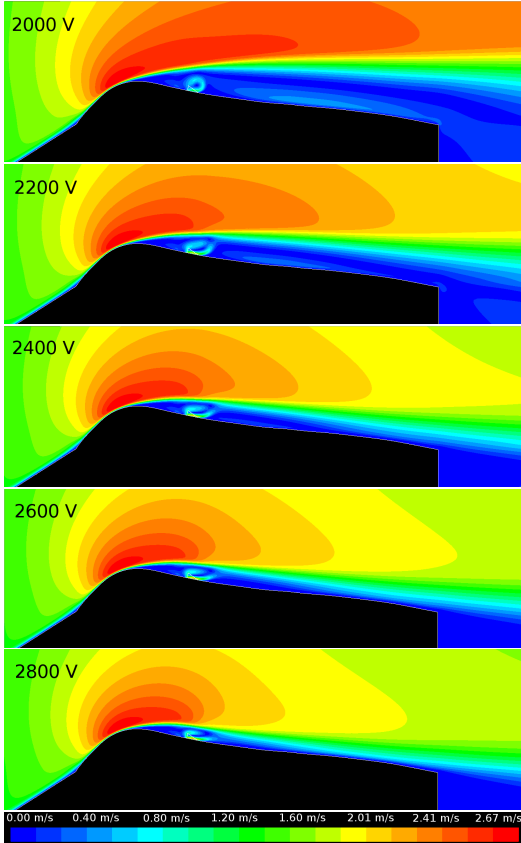Table 1. Plasma actuator properties used in the numerical simulation



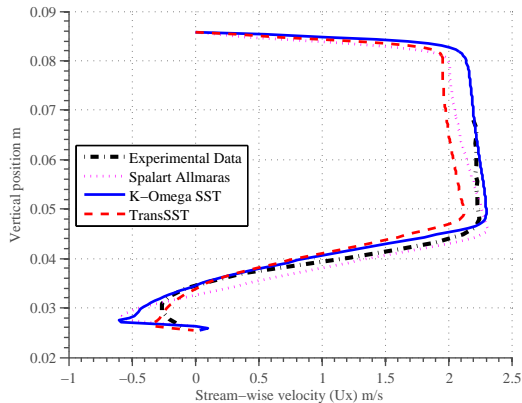Figure 4. Velocity distributions with plasma voltage varied from 2000 V to 2800 V (Plasma-on)



Figure 5. Comparison of streamwise velocity profiles for various turbulence models at Station 2 (Plasma-off baseline case)

| Voltage | Selected Alpha Value ($\alpha$) |
|---|---|
| 2000 V | 0.2 |
| 2200 V | 0.6 |
| 2400 V | 0.6 |
| 2600 V | 0.6 |
| 2800 V | 0.6 |

Table 2. Calibrated alpha ($\alpha$) values

solution in terms of computational expense and solution convergence. The shearing layer between flow recirculation from the airfoil surface and freestream velocity is approximately the same height as the experimental data (45 mm above airfoil surface). The freestream velocity, which Matsunuma and Segawa [5] describe as approximately 2.25 m/s, proved slower in the 2D numerical simulations. This has been attributed to additional flow contraction due to the boundary layers on the side walls in the wind tunnel, which are not considered in computation, and correction is made for the velocity by taking into account the ratio of the massflow rate between experiment and CFD, as $U_{x_{normalized}} = U_{x_{CFD}}(\dot{m}_{CFD}/\dot{m}_{Experimental})$.

Plasma Actuator Calibration

Calibration of the plasma actuator model is completed through variation of the $\alpha$ value of 0.2, 0.4, 0.6, and 0.8 for each voltages recorded by Matsunuma and Segawa [5]: 2000 V, 2200 V, 2400 V, 2600 V, and 2800 V.

From Equation (3) and (4), $\alpha$ acts directly proportional to the plasma actuator strength and injection of momentum into the plasma-on region. Figure 6 shows as a result the linear increase in injection of momentum acts to reduce the recirculation zone and shorten the reattachment point along the airfoil in the chord direction. Figure 6 shows a sample plot with various $\alpha$ values for the input voltage 2400 V. The $\alpha$ value of 0.6 has been consequently chosen due to qualitative agreement for with good estimation of freestream and recirculation velocity profiles as well as shear layer height. The effect of massflow continuity is well illustrated in Figure 6. As the value of alpha and hence the plasma strength are increased, the freestream velocity decreases due to lower flow contraction and reduced height of the recirculation region. For all plasma-on cases $\alpha$ values are qualitatively selected and listed in table 2.

Turbulence intensity profiles are also presented so as to gain insight into the comparison between experimental and CFD flowfields. Figure 7 shows a sample of the collected turbulence intensity plots. The experimental turbulence intensity is significantly higher and lower than those predicted by CFD through steady-state simulations. The most important characteristics for calibration are the shear layer height, which is also modeled well by the sharp change in turbulence intensity at approximately 38 mm, and the increase in turbulence intensity describing the unsteady vortex shedding nature inside the recirculation
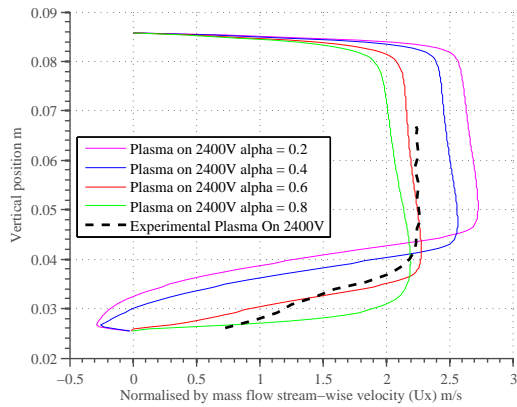
Figure 6. Plasma-on at 2400V - Streamwise velocity at Station 2 (0.0991 m)
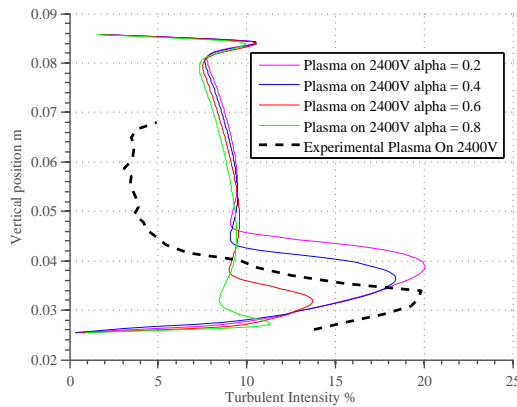
and reattachment zone.



Figure 7. Plasma-on at 2400V - Streamwise turbulence intensity at Station 2 (0.0991 m)

Estimation Of Total Pressure Loss Coefficient

The total pressure coefficient is calculated to assess the effectiveness of plasma flow control, defined as the mass-averaged total pressure at Station 2 normalized by the freestream dynamic pressure. The total pressure loss coefficient is calculated by the difference between pressure coefficients at station 1 and 2.

$$C_{p0} = \frac{\rho |U| P_0}{\frac{1}{2}\rho\, U_\infty^2} \quad (5)$$

Figure 8 shows the reduction of total pressure loss coefficient with increasing input voltage. Matsunuma and Segawa use an empirical formula to calculate the total pressure loss coefficient ($C_{P0}$) between Station 1 and 2, based on separation displacement height. The agreement in pressure loss reduction is strongly illustrated between both CFD and experiment. The total pressure loss coefficients predicted by CFD are higher than those calculated by Matsunuma and Segawa, however the percentage reduction trend and gradient between baseline plasma-off case and plasma-on cases agree well.

**Conclusions and Future Work**

Using experimental data generated by Matsunuma and Segawa [5], a numerical study has been conducted for the baseline and plasma-on cases. Reasonable agreement has been observed for the velocity and turbulence intensity profiles at the trailing edge. The plasma actuator model was calibrated qualitatively
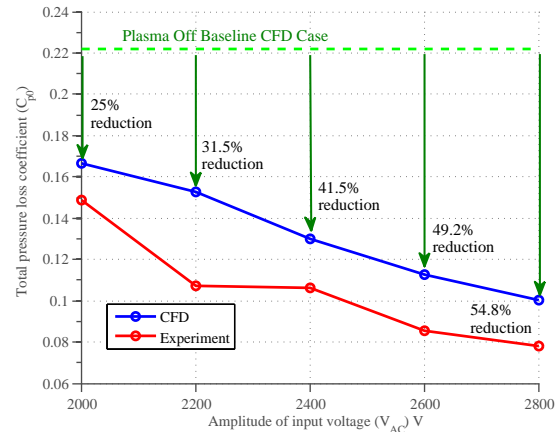


Figure 8. Reduction in total pressure loss coefficient for CFD compared to experiment vs. input voltage

| Voltage | Experimental data [5] | CFD prediction |
|---------|----------------------|----------------|
| 2000 V | 13 % | 25.0 % |
| 2200 V | 38 % | 31.5 % |
| 2400 V | 37 % | 41.5 % |
| 2600 V | 50 % | 49.2 % |
| 2800 V | 55 % | 54.8 % |

Table 3. Percentage reduction in pressure loss coefficient ($C_{P0}$)

for steady state conditions using RANS simulations, resulting in favorable agreement for total pressure savings owing to separation control with plasma actuators.

Following the development of the calibrated and validated DBD model described in this paper, a design optimization study is to be undertaken including (1) plasma actuator size, orientation, and location (2) voltage amplitude (3) optimization of configurations for various Reynolds numbers, by means of surrogate-assisted evolutionary algorithms.

**References**

[1] Andersson, A., Jayaraman, B., & Shyy, W., Modeling of glow discharge-induced fluid dynamics, *Journal of Applied Physics*, **92**, 2002, 6434.

[2] Corke, T., & Post, M., Overview of Plasma Flow Control: Concepts, Optimization, and Applications, *43rd AIAA Aerospace Sciences Meeting and Exhibit*, 2005.

[3] Corke, T.C., Huang, J. & Thomas, F.O., Plasma Actuators for Separation Control of Low-Pressure Turbine Blades, *AIAA Journal*, **44**, 2006, 51-57.

[4] Fasel, H.F. & Gross, A., Numerical Investigation of Low-Pressure Turbine Blade Separation Control, *AIAA Journal*, **43**, 2005, 2514-2525.

[5] Matsunuma, T., & Segawa, T., Effects of Input Voltage on Flow Separation Control for Low-Pressure Turbine at Low Reynolds Number by Plasma Actuators, *International Journal of Rotating Machinery*, 2012, 1-10.

[6] Rizzetta, D.P., & Visbal, M.R., Large-Eddy Simulation of Plasma-Based Turbulent Boundary-Layer Separation Control, *AIAA Journal*, **48**, 2010, 2793-2810.